Thermal analysis of Double Stator Switched Reluctance Machine (DSSRM) Using Finite Element Method

[1]Mohammadali ABBASIAN [2]Hadi.JALALI
1.Department of Electrical and Computer Engineering, Khorasgan Branch, Islamic Azad University P.O. Box81595-158
Isfahan, Iran, Phone: +989335730756, Fax: +983135354060
2.Department of Electrical Engineering, Khomeinishahr Branch, Islamic Azad University P.O.Box 84175-119
Isfahan, Iran, Phone: +989335730756, Fax: +983112305575
Email: m.abbasian@khuisf.ac.ir , hadi.jalali@iaukhsh.ac.ir

Abstract: *Double Stator Switched Reluctance Machine (DSSRM) is known as a new Switched Reluctance Machine (SRM) having two stators and one rotor. This machine enjoys a short magnetic flux path and high power/torque density. DSSRM is a non conventional machine yielding limited information about heat dissipation, thereby making thermal analysis an essential stage for this new machine. This study, using finite element method (FEM), employs the two dimensional (2-D) thermal analysis of Double Stator Switched Reluctance machine (DSSRM) in order to observe real heat distribution in the parts of the machine. Electromagnetic losses forming the heat source are calculated. A 2-D thermal analysis is done to observe the temperature distribution and maximum temperature for a rotation speed of 1000 RPM. Accordingly, simulation results for an 8/6 DSSRM are presented.*

Key words: *Double Stator Switched Reluctance Machine (DSSRM), Thermal Analysis, Computational Fluid Dynamics (CFD), Finite Element Method (FEM).*

1. Introduction.

During the design stage of electrical machines, a serious problem encountered is the determination of the temperature distribution in different parts of the machine. It is known that the electric currents and friction in an electric machine generate heat. If there is a temperature rise in different parts of the machine, it can cause the deterioration of insulation in windings [1], leading to machine failure.

With the growing demand for the development of smaller and more efficient electric machines, a trend has emerged to carry out a precise thermal analysis along with the traditional electromagnetic design. This makes it necessary to create accurate thermal models for the machines and obtain the distribution of temperature in them .

In an electrical machine, it is known that the calculation of the maximum continuous rating needs an adequate thermal model to ensure that the cooling provision is sufficient to avoid overheating since the torque density is thermally limited [2]. In addition, the stator temperature can influence the efficiency because the resistivity of the copper windings is increased with temperature.

Switched reluctance machines are doubly-salient singly excited reluctance machines. They have salient poles on both rotor and stator sides, without any excitation windings, magnets, or cage winding on the rotor [3]. SRM drive systems have received attention for automotive, defense and aerospace applications requiring ruggedness, high speed capability, and fault tolerance. However, they have some problems such as a high level of vibration and acoustic noise, large torque ripple, and low torque per unit volume in comparison to permanent magnet machines [4].

In recent years, many attempts have been made to address thermal analysis of the SRM. In a study, a lumped parameter thermal model for SRM was used [5]. The lumped parameter thermal model is known as one of the most popular methods for estimating the temperature rise with internal losses. According to this method, from the thermal point of view, the system can be divided into several parts connected to each other by means of thermal resistors and capacitors. In [6], a Lumped thermal model for switched reluctance machine was introduced too. A thermal analysis of SRM using Soft magnetic composite (SMC) materials was introduced in [7].

For further accuracy, the thermal analysis of SRM can be performed by Finite Element Method (FEM) [8]. A precise thermal analysis of SRM by FEM was presented in [9]. On the other hand, a thermal analysis of SRM was introduced in [10]. In that study, to estimate the distribution of air velocity and the coefficient of convection at different heat dissipating surfaces in the inner part of SRM , a computational fluid dynamics (CFD) flow analysis procedure was done. In [11] a analysis the thermal effects due to copper losses and iron losses in a 6/4 SRM by the 2-D FEM is done. In [12] a thermal modeling of electric machines was introduced using the lumped parameter and limited CFD analysis . Since this motor's structure is new, it is not possible to perform a wide thermal analysis for its real model. Therefore, more advanced techniques such as CFD are

required to further investigate the thermal effects in electrical machines [13]. CFD has the advantage that it can be used to predict flow in complex regions, as in around the machine windings [14].

Double stator switched reluctance machine (DSSRM) is a new SRM designed to perform at high torque levels [15]. This machine benefits from two stators made of laminated ferromagnetic material and equipped with concentrated windings. They are positioned on the interior and exterior of a cylindrical rotor. The rotor is formed by segments held together using a non ferromagnetic cage. The cross section of a 4-phase 8/6 DSSRM can be seen in Figures 1 and 2 .

The inner stator of DSSRM is surrounded by the cylindrical rotor, causing limitation in the heat dissipation of the inner stator windings. So, considering the effect of rotor topology in the heat transfer of this machine is necessary. In this paper, the temperature rise analysis of DSSRM was conducted using FEM. The geometrical model of the DSSRM was developed as a parametric model and the simulation results obtained from CFD were presented for a 8/6 DSSRM, as shown in Table 1.

Table 1. Parameters of the DSSRM [15]

No. of phases	4
No. of stator/rotor poles	8/6
Outer radius of outer stator	72.0
Outer radius of inner stator	43.9
Rotor segment thickness [mm]	9.0
Air gap	1.0
Stack length [mm]	115.0
Arc of the rotor [deg.]	47
Turns per coil	50
[Ω] Resistance @ 20°C	0.78
Rated speed of motor [rpm]	1000
Wire	AWG14

2. Temperature analysis of DSSRM.

A two dimensional (2-D) model of DSSRM used in this study can be seen in Figure 1. The machine parameters are shown in Table I. The model consisted of two stators, one rotor, two stator windings and two airgaps.

It must be noted that drawing the geometrical model of the machine can be a time-consuming task, especially if different designs have to be considered. Therefore, the geometrical model was created as a parametric model and mesh generation was applied.

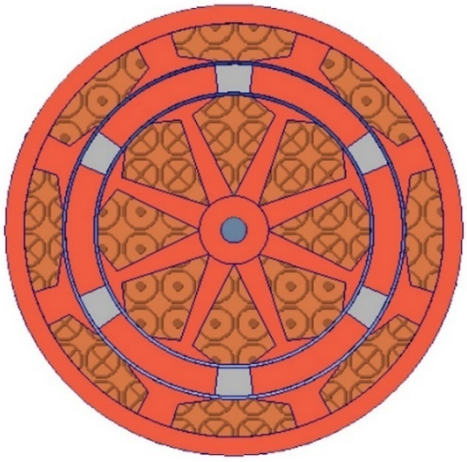

Fig. 1. Geometrical model of 8/6 DSSRM

Core losses in the laminations and copper losses in the windings are the two main components of electromagnetic losses in DSSRM. These losses are known as the heat source in a thermal analysis [16]. Core losses in DSSRM machine were relatively low, due to the benefits from a short flux path.

Accordingly, the copper loss for inner and outer stators and rotor for single pulse control mode of DSSRM at a speed of 1000 RPM could be calculated. Machine losses for two different currents were calculated and the rate of Q (w/ m^3) was the main heat source as summarized in Table 2. A 2-D Finite element model of DSSRM is shown in Figures 3 and 4.

Table 2. Quantity of heat generation

Rotational speed [rpm]	1000	
	I=5A	I=10A
Heat generation inner winding(w/m^3)	193338.24	959019.2
Heat generation outer winding(w/m^3)	227250.88	1127236.8
Heat generation inner stator (w/m^3)	17294.22	84174.35
Heat generation outer stator (w/m^3)	8493.444	41339.25
Heat generation rotor (w/m^3)	53476.734	242903.88

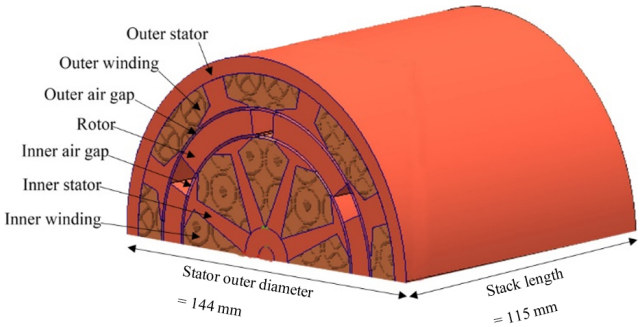

Fig.2. Geometry of the DSSRM

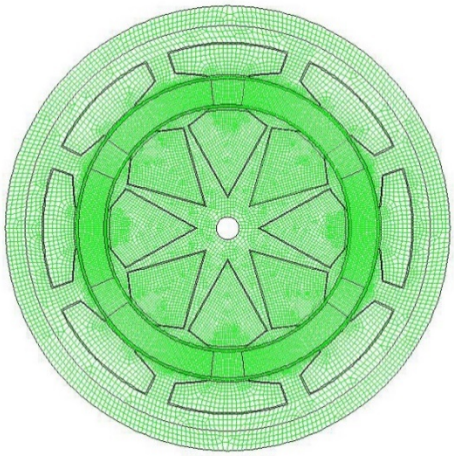

Fig. 3. 2-D Finite element model of the DSSRM

To predict the temperature distribution in components of machine , a thermal analysis of DSSRM was proposed using FEM. For heat transfer through the external surface of the machine, both natural and forced convection could be considered. Due to the rotation of the rotor heat transfer from stator and windings to airgap could be modeled by forced convection. The thermal parameters used in the analysis can be seen in Table 3.

Table 3. Thermal parameters [18] , [19]

	Thermal conductivity $(W/m/^{\circ}C)$	Specific heat $(J/kg/^{\circ}C)$	Density (kg/m^3)
Stator lamination (iron)	20	438	7650
Copper	401	385	8933
Slot liner	0.076	1172	2150
Air	0.0263	1007	1.16
Frame (aluminum)	177	875	2770
Slot wedge	0.29	1172	2150

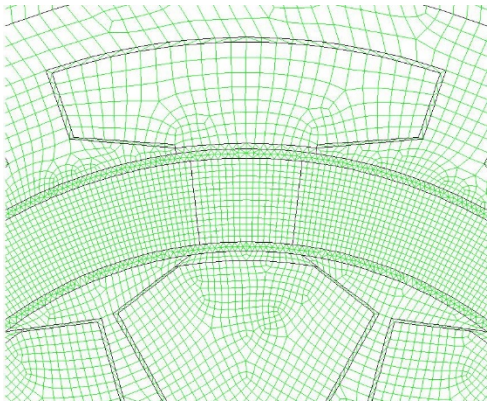

Fig. 4. Meshed model of the DSSRM

It has been shown that the windings of the electrical have complex structure. Therefore, it is not possible or appropriate to model the position of each individual conductor during thermal analysis.

One approach that can be employed to simplify the model is the use of an equivalent thermal conductivity of the system windings and insulation by various methods such as the analytical method, experiments or FEM.

It can be defined as [17]:

$$K_{cu,ir} = 0.2425\left[\left(1-k_f\right)A_{slot}L_{core}\right]^{-0.4269} \quad (1)$$

where $k_{cu,ir}$ is the equivalent thermal conductivity of the insulation material and air in the stator slots, k_f is the slot filling factor, A_{slot} is the area of slot and L_{core} is the axial core length.

This coefficient is usually in a range from 0.6 to 0.9 W/m.◦C depending on filling factor and winding configuration [18], [20],[21]. By using the numerical and analytical methods, an equivalent thermal conductivity of 0.80 W/m.◦C can be considered in the proposed thermal analysis for the windings.

3. Simulation result analysis.

In thermal analysis with various boundary conditions, conductive heat transfer can be obtained from the Fourier law as shown below:

$$\frac{1}{r}\frac{\partial}{\partial r}\left(k_r\frac{\partial T}{\partial r}\right)+\frac{1}{r^2}\frac{\partial}{\partial \theta}\left(k_\theta\frac{\partial T}{\partial \theta}\right)+\frac{\partial}{\partial Z}\left(k_z\frac{\partial T}{\partial z}\right)+\dot{q} \quad (2)$$

In this study, since solution is 2-D , the effect of thermal change in direction of rotor axis could be ignored.

$$\frac{1}{r}\frac{\partial}{\partial r}\left(k_r\frac{\partial T}{\partial r}\right)+\frac{1}{r^2}\frac{\partial}{\partial \theta}\left(k_\theta\frac{\partial T}{\partial \theta}\right)+\dot{q} \quad (3)$$

Dimensionless of numbers which employed in the calculation of convection heat transfer coefficients are [22], [23]:

Reynolds number:

$$R_e = \frac{\rho v L}{\mu} \quad (4)$$

where ρ is the fluid density, μ is the fluid dynamic viscosity, υ is the fluid velocity and L is the characteristic length of the surface.

Grashof number:

$$G_r = \frac{\beta g \theta \rho^2 L^3}{\mu^2} \quad (5)$$

where β is the coefficient of cubical expansion of fluid , g is the gravitational force of attraction and θ is the temperature difference between the surface and the fluid.

Prandtl number:

$$P_r = \frac{C_p \mu}{\lambda} \quad (6)$$

where C_p is the specific heat capacity of the fluid and λ is the thermal conductivity of the fluid.

Nusselt number:

$$N_u = \frac{hL}{\lambda} \quad (7)$$

Nusselt number usually is used for the calculation of the convection heat transfer coefficient h(w/m^2.◦C)

$$h = \frac{\lambda N_u}{L} \quad (8)$$

The general form of convection correlation for natural convection is:

$$N_u = a\left(G_r P_r\right)^2 \quad (9)$$

The general form of convection correlation for forced convection is:

$$N_u = a\left(R_e\right)^b \left(P_r\right)^c \quad (10)$$

where a, b and c are constants.

$G_r P_r = R_a$ is the Rayleigh number.

In a forced convection system, the value of Re determines if there is laminar or turbulent flow. It is specified by $G_r P_r$ product in the natural convection system.

For laminar flow (R_e <5*10^5) and (0.6< P_r <50)

For turbulent flow (R_e >5*10^5)

By assuming a value of 4 m/s for the air velocity over frame, the forced convection coefficient over this surface is estimated to be 30 w/m^2.◦C. It should be noted that as the convection coefficients are rather low, heat transfer by radiation could be important when only natural convection for the external surfaces of the machine is considered in the thermal analysis. When we consider the inside air, temperature rise can be obtained for h = 30 w/m^2.◦C in the 2-D thermal analysis of the 8/6 DSSRM. For all thermal simulation results, the external surface of the machine (frame) is 30 w/m^2.◦C . Different types of boundary conditions can be seen in Figure 5.

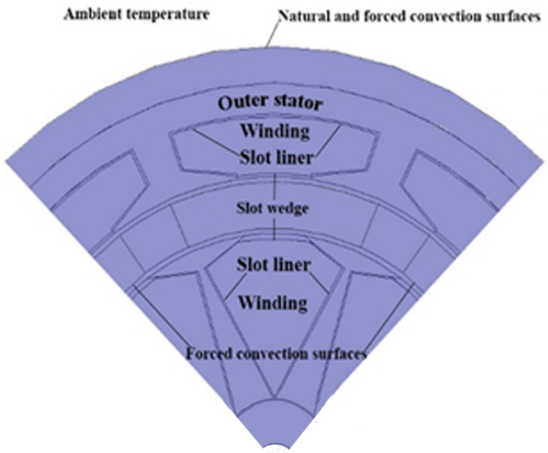

Fig.5. Different types of boundary conditions and machine geometrical model in thermal analysis

Thermal analysis was carried out for two different currents (Table 4). Accordingly, the results of CFD for the thermal analysis was obtained over 140 hours using 8 processors on a Linux cluster with 2.2 GHz. Table IV represents the summary of thermal analysis performed in the inner windings on the machine in two different currents. For the thermal analysis ANSYS Fluent [24] has been used.

Table 4 . Results of thermal analysis for different times inner winding

Time (min)	Maximum Temperature(°C)	
	I = 5 A	I = 10 A
10	27.09553	54.95753
50	44.52153	140.54845
100	55.8473	196.16202
150	61.24696	222.67468
200	63.8181	235.29911
250	65.04219	241.30991
300	65.62452	244.1694

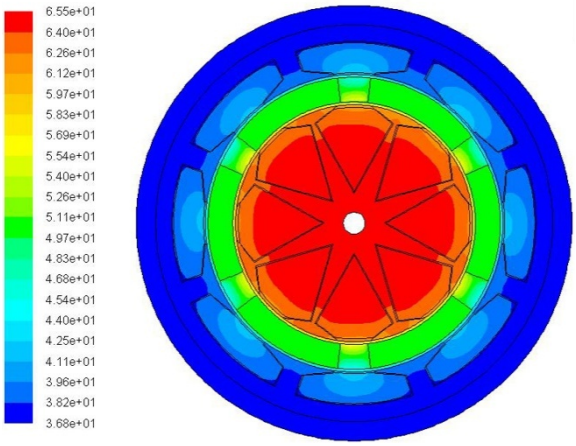

Fig. 6. Temperature distribution at 1000 RPM in I = 5 A

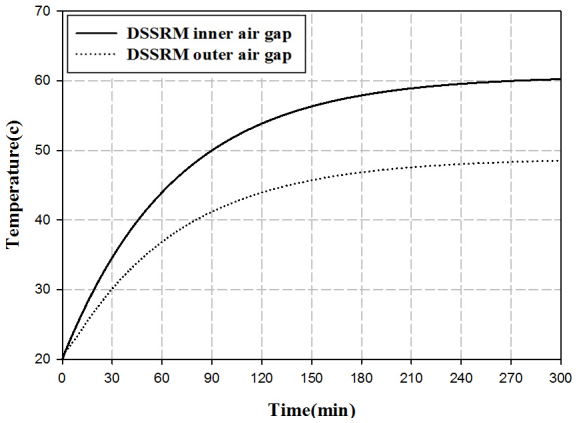

Fig. 7. Temperature-time curve in Air gap in I = 5A

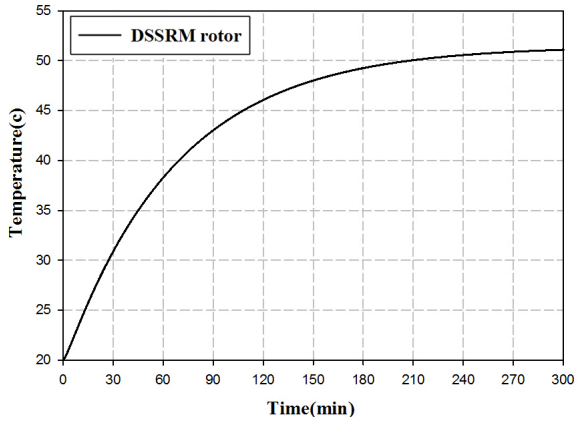

Fig. 8. Temperature-time curve in Rotor in I = 5A

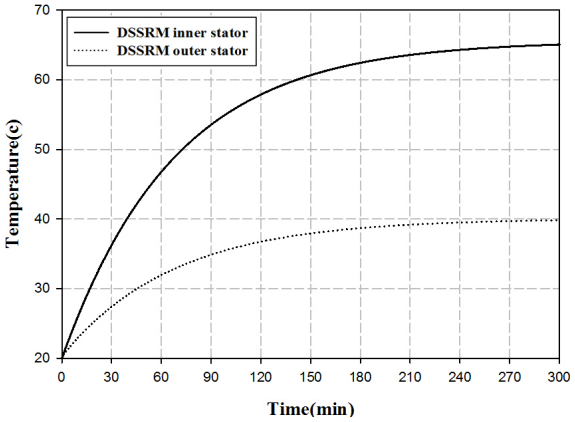

Fig. 9. Temperature-time curve in Stator in I = 5A

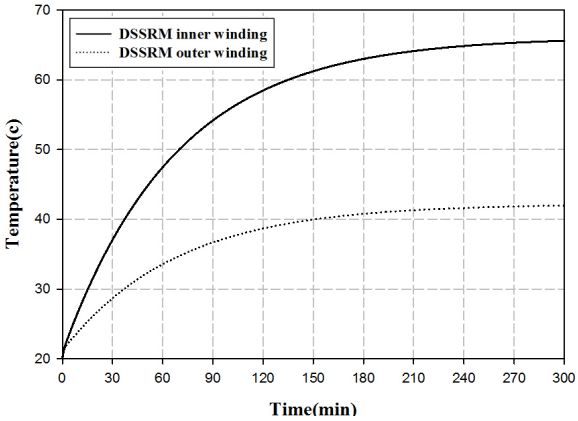

Fig. 10. Temperature-time curve in Winding in I=5A

Figures 6 to 10 show the results of thermal analysis in I=5A . Figure 6 represents temperature distribution in machine while Figures 7 to 10 show temperature in different parts of the machine at 1000 RPM. From Figure 6, it can be seen that at 1000 RPM, the hot spot temperature is 65.5ºC, occurring in the inner winding.

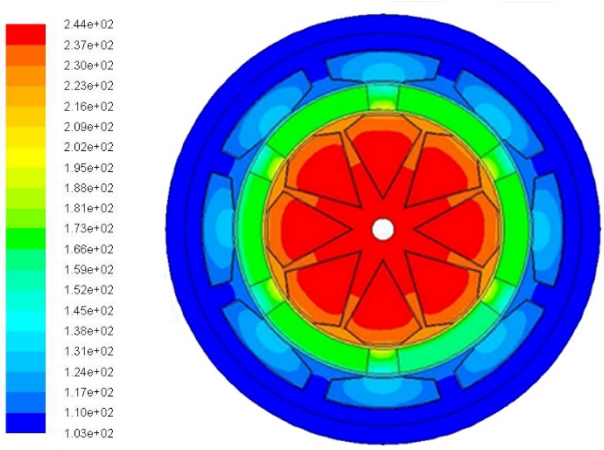

Fig. 11. Temperature distribution at 1000 RPM in I = 10 A

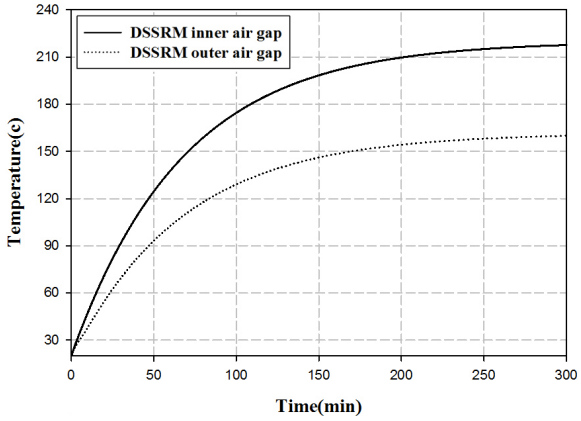

Figure 12. Temperature-time curve in Air gaps in I=10A

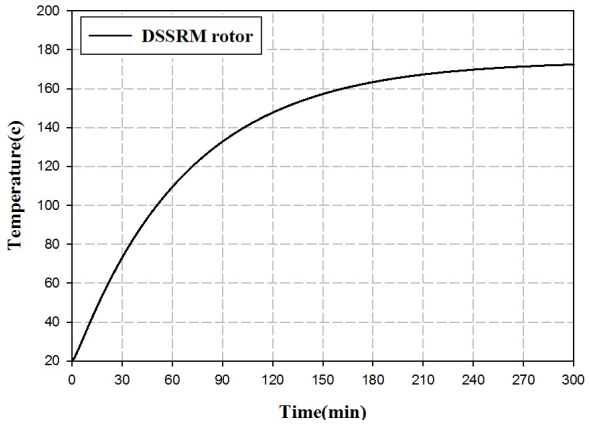

Figure 13. Temperature-time curve in Rotor in I=10A

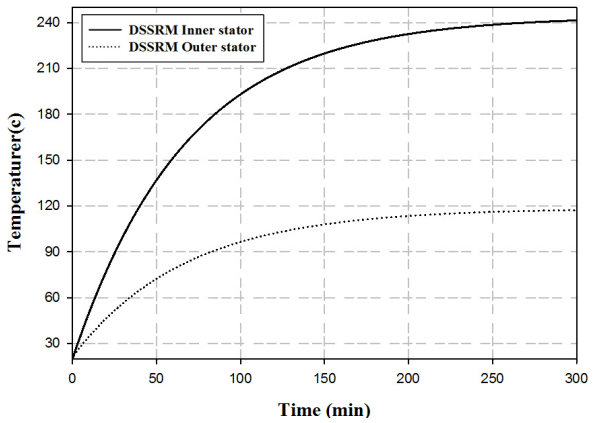

Figure 14. Temperature-time curve in Stator in I=10A

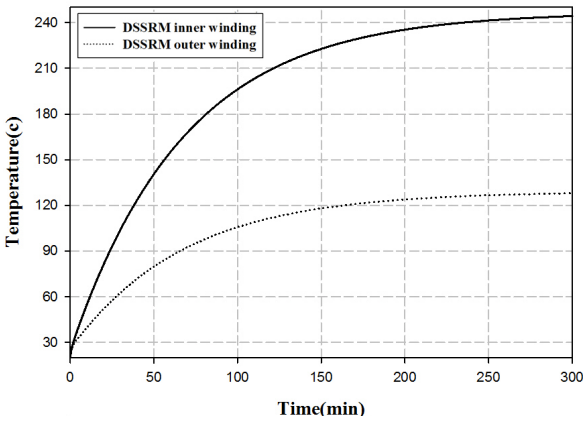

Figure 15. Temperature-time curve in winding in I=10A

Figures 11 to 15 show the results of thermal analysis in I=10A Temperature distribution in machine can be seen in Figure 11. On the other hand, Figures 12 to 15 illustrate temperature in different parts of the machine at 1000 RPM. From Figure 11, it can be seen that at 1000 RPM, the hot spot temperature is 244ºC, occurring in the inner winding.

4. Conclusion

This paper presented a 2-D FEM temperature analysis of DSSRM using ANSYS Fluent software. The maximum temperature of the machine was obtained after 300 minutes in two different currents. It was found that increasing the temperature in a machine could damage the insulation of the coil, which, in turn, caused unauthorized thermal stress, noise sound, reduced efficiency and even change in authorized tolerance. Therefore, in designing a machine, it is important to ensure that maximum temperature would not reach the critical temperature. Practically, on the basis of empirical evidence obtained, one can say that the winding insulation life is decreased with temperature at the rate of about 50% for every 10° C insulating temperature rise, but, it should be explained that depending on their duration, intermittent periods at higher than normal temperature can be tolerated. This wire (with insulation Polystermid Polyamide - Imide (PEI+PAI)) can operate at temperatures ranging 240°C from 300°C for intermittent duty. So, according to the above description, the insulation class of windings, slot liners and slot wedges and the costs involved, this machine can work with currents not higher than 10A.

References

1. J. Faiz, A. Dadgari.: Heat distribution and thermal calculations for a switched reluctance motor, Journal of Electrical and Electronics Engineering, Australia. In: IE Australia & IREE Australia 12 (4) (1992) 349–361.

2. David A. Howey , Peter R. N. Childs, and Andrew S. Holmes.: Air-Gap Convection in Rotating Electrical Machines. In IEEE TRANSACTIONS ON INDUSTRIAL ELECTRONICS, VOL. 59, NO. 3, MARCH 2012.
3. T. J. E. Miller.: Switched Reluctance Motors and their control. In Oxford Science Publications, 1993.
4. P.J. Lawrenson ,J.M. Stephenson ,P.T. Blenkinsop , J. Corda ,N.N. Fulton.: variable-speed switched reluctance motors. In: IEE Proceedings B (Electric Power Applications),Volume 127, Issue 4, July 1980.
5. J. Faiz, R. Iranpour, and P. Pillay.: Thermal model for a switched reluctance motor of TEFC design during steady and transient operation. In: Elect. Mach. Power Syst., vol. 26, no. 1, pp. 77–91, Jan. 1998.
6. H. Rouhani, J. Faiz, C. Lucas.: Lumped thermal model for switched reluctance motor applied to mechanical design optimization. In: Mathematical and Computer Modelling, Volume 45, Issues 5–6, March 2007, Pages 625-638.
7. K. Vijayakumar, R. Karthikeyen and R. Arumugam.: Analysis and characterization of a switched reluctance machine using soft magnetic composite material. In: Journal of Electrical Engineering (2011), Vol. 11.
8. W. Wu, J. B. Dunlop, S. J. Collocott, and B. A. Kalan.: Design optimization of a switched reluctance motor by electromagnetic and thermal finite element analysis. In: IEEE Trans. Magn., vol. 39, no. 5, pp. 3334–3336, Sep. 2003.
9. S. Inamura, T. Sakai, and K. Sawa.: A temperature rise analysis of switched reluctance motor due to the core and copper loss by FEM. In: IEEE Trans. Magn., vol. 39, no. 3, pp. 1554–1557, May 2003.
10. K. N. Srinivas and R. Arumugam.: Analysis and characterization of switched reluctance motors: Part 2 - Flow, thermal and vibration analyses. In: IEEE Trans. Magn., vol. 41, no. 4, pp. 1321–1332, Apr.
2005.
11. S. Badache and A . Taieb Brahim.: Thermal Phenomena analysis of 6/4 Switched Reluctance Machine by the 2D Finite Elements Method. In: Journal of Electrical Engineering (2013), Vol. 13.
12. Shafigh Nategh, ZheHuang, Andreas Krings, Oskar Wallmark and Mats Leksell .: Thermal Modeling of Directly Cooled Electric Machines Using Lumped Parameter and Limited CFD Analysis. In: IEEE TRANSACTIONS ON ENERGY CONVERSION, VOL. 28, NO. 4, DECEMBER 2013.
13. C. Kral, A. Haumer, M. Haigis, H. Lang, and H. Kapeller.: Comparison of a CFD analysis and a thermal equivalent circuit model of a TEFC induction machine with measurements. In: IEEE Trans. Energy Convers.,vol. 24, no. 4, pp. 809–818, Dec. 2009.
14. J. D. Anderson, Jr.: Computational Fluid Dynamics: McGraw-Hill, International Editions, 1995.
15. Abbasian, M., Moallem, M., Fahimi, B.: Double-Stator Switched Reluctance Machines(DSSRM): Fundamentals and Magnetic Force Analysis. In: IEEE Trans. on Engery Conversion, vol.25 no.3, pp.589-597, 2010.
16. J. Faiz, B. Ganji, C. E. Carstensen, K. A. Kasper, and R. W. D. Doncker.: Temperature Rise Analysis of Switched Reluctance Motors Due to Electromagnetic Losses. In: IEEE Trans. Magn, vol. 45, no. 7, July 2009.
17. D. Staton, A. Boglietti, and A. Cavagnino.: Solving the more difficult aspects of electric motor thermal analysis in small and medium size industrial induction motors. In: IEEE Trans. Energy Convers., vol. 20, no. 3, pp. 620–628, Sep. 2005.
18. W. Wu, J. B. Dunlop, S. J. Collocott, and B. A. Kalan.: Design optimization of a switched reluctance motor by electromagnetic and thermal finite element analysis. In: IEEE Trans. Magn., vol. 39, no. 5, pp. 3334–3336, Sep. 2003.
19. F. Incropera and D. DeWitt.:Fundamentals of Heat and Mass Transfer, New York: Wiley, 1990.
20. J. F. Trigeol, Y. Bertin, and P. Lagonotte.: Coupling control volumemodeling in fluid and lumped thermal model - Application to an inductionmachine. In: in Proc. IECON'06, Nov. 2006, pp. 4829 4834.
21. C. E. Carstensen.: Eddy Currents in Windings of Switched ReluctanceMachines. Ph.D dissertation, RWTH Aachen, Aachen, Germany, 2007.
22. D. A. Staton and A. Cavagnino.: Convection Heat transfer and Flow Calculations Suitable for Electrical Machines Thermal Models. In: IEEE trans. Industrial Electronics, vol. 55, no. 10, 2008.
23. D. A. Staton and A. Cavagnino.: Convection Heat transfer and Flow Calculations Suitable for Analytical Modelling of Electrical Machines. In: IEEE Annual conference on Industrial Electronics, pp. 4841-4846, Nov 2006.
24. Ansys Fluent Package.[Online]. Available: www.ansys.com.